Magnetic field driven topological transitions in the noncentrosymmetric energy spectrum of the two-dimensional electron gas with Rashba-Dresselhaus spin-orbit interaction

I. V. Kozlov and Yu. A. Kolesnichenko*

B. Verkin Institute for Low Temperature Physics and Engineering of the National Academy of Sciences of Ukraine, 47 Nauky Avenue, Kharkiv 61103, Ukraine

(Received 2 October 2018; published 19 February 2019)

Two-dimensional (2D) electron systems with a combined Rashba and Dresselhaus spin-orbit interaction (SOI) having a complicated energy spectrum with a conical point and four critical points are promising candidates to observe electron topological transitions. In the present paper we have investigated the evolution of the electron spectrum and isoenergetic contours under the influence of a parallel magnetic field. General formulas for the energies of critical points for arbitrary values of SOI constants and magnetic field are found. The existence of critical magnetic fields at which a number of critical points is changed has been predicted. The magnetic field driving topological Lifshitz transitions in the geometry of isoenergetic contours has been studied. Van Hove's singularities in the electron density of states are calculated. The obtained results can be used for theoretical investigations of the different electron characteristics of such 2D systems.

DOI: 10.1103/PhysRevB.99.085129

I. INTRODUCTION

In a fundamental paper [1], Lifshitz predicted "electron transitions," abrupt changes of the Fermi surface topology under the continuous variation of some parameters, such as pressure, chemical potential, etc. These transitions result in anomalies in the different kinetic and thermodynamic characteristics of metals that have stipulated special attention to their detailed investigations (see Refs. [2–4] for a review). In recent years the interest in Lifshitz transitions has become renewed in view of intensive studies of new electron systems, such as graphene, topological insulators, semimetals, superconductors, Dirac semimetals, and Weyl semimetals, in which different types of electron topological transitions take place [5]. Low-dimensional systems with a spin-orbit interaction (SOI) [6,7] are possible candidates to observe topological transitions in the energy spectrum as well. Manifestations of topological transitions in a magnetic susceptibility of three-dimensional (3D) semiconductors with SOI had been predicted by Boiko and Rashba [8]. Recently, enhanced orbital paramagnetism related to the topological transition was observed in a layered semiconductor BiTeI when the Fermi energy E_F is near the crossing point of the Rashba spin-split conduction bands [9].

Among a variety of spin-orbit materials, two-dimensional (2D) systems made of zinc-blende III-V, wurtzite, SiGe semiconductors, semiconductor quantum wells, etc., occupy a special place possessing a combined Rashba-Dresselhaus (RD) SOI [10–13] (see Ref. [14] for a review). The interplay between two types of SOI results in anisotropic spin-split Fermi contours which lead to an anisotropic magnetoresistance [15,16], an enhancement of electron propagation along a narrow range of real-space angles from an isotropic source [17], anisotropic Friedel oscillations [18,19], and so on.

In the presence of SOI a parallel magnetic field **B** results not only in the appearance of a Zeeman energy but is also affects the dispersion law of charge carriers [20], changing the geometry and breaking the central symmetry of 2D Fermi contours [21]. A possible way to manage the anisotropy of the transport characteristics seems to be promising for practical applications. The energy spectrum of 2D electrons with RD SOI in the in-plane magnetic field **B** can be easily obtained, but to date the information on the evolution of the energy branches with the changes of direction and an absolute value of vector **B** is incomplete and disconnected [22–24]. In a recent paper [25] an electronic transport in 2D electron gas subjected to an in-plane magnetic field for the case of Rashba SOI had been studied theoretically. Singularities of a conductivity and a spin polarization as functions of the Fermi level or magnetic field, which occurs when the Fermi level passes through the Van Hove singularity [26], were analyzed. It was predicted that the transport anisotropy dramatically changes near the singularity. Such anisotropy was reported in an experiment [27].

In this paper we present a consistent consideration of changes in the energy spectrum of 2D electrons with RD SOI under the variations of the parallel magnetic field. Special attention will be paid to magnetic field induced 2D electron topological transitions. The structure of the paper is as follows. Section II contains some known information which is the basis of subsequent investigations. We present the Hamiltonian of the system, and its eigenvalues and eigenfunctions. The energy spectrum in the absence of the magnetic field is discussed from the point of view of the possibilities of topological transitions. In Sec. III, the evolution of the energy spectrum for an arbitrary value and direction of vector **B** is studied. We predict the existence of critical fields B_{c1} and B_{c2}

*kolesnichenko@ilt.kharkov.ua

at which the number of critical points (minima and saddle points) of the energy surfaces is changed. So, a possibility appears to create artificial degenerate critical points of the energy spectrum. Limiting cases of weak and strong magnetic fields are considered. In Sec. IV, as examples, we present explicit analytical results for the energies of the critical points, their position in $\mathbf{k}$ space, and critical values B_{c1} and B_{c2} for the magnetic field directed along the symmetry axes. Variations of the topology of isoenergetic contours, which are a 2D analog of the Fermi surface, under variations of the magnetic field are analyzed in Sec. V. In Sec. VI, the singular part of the electron density of states is discussed. The obtained formulas allow us to determine SOI constants from Van Hove singularities [26]. We conclude the paper with some final remarks and a summary of main results in Sec. VII.

II. HAMILTONIAN OF THE SYSTEM: ENERGY SPECTRUM AT ZERO MAGNETIC FIELD

Our calculations are based on the widely used model of the 2D single-electron Hamiltonian taking into account the linear terms of RD SOI (see, for example, Refs. [15,17,18,22,23,28–31]),

$$\hat{H}_0 = \frac{\widehat{\mathbf{P}}^2}{2m}\sigma_0 + \frac{\alpha}{m}(\sigma_x\widehat{P}_y - \sigma_y\widehat{P}_x) + \frac{\beta}{\hbar}(\sigma_x\widehat{P}_x - \sigma_y\widehat{P}_y) - \frac{g^*}{2}\mu_B\mathbf{B}\sigma. \quad (1)$$

Here, $\widehat{\mathbf{P}} = \widehat{\mathbf{p}} + e\mathbf{A}/c$ is the operator of the generalized momentum, $\widehat{\mathbf{p}} = \hbar\widehat{\mathbf{k}} = -i\hbar\nabla = (\widehat{p}_x, \widehat{p}_y)$ is the operator of the in-plane momentum, $\mathbf{A}$ is the vector potential of the in-plane magnetic field $\mathbf{B} = (B_x, B_y, 0)$, m is an effective electron mass, $\sigma_{x,y,z}$ are Pauli matrices, $\sigma = (\sigma_x, \sigma_y, \sigma_z)$ is the Pauli vector, $\hat{\sigma}_0$ is a 2×2 unit matrix, α and β are Rashba (α) [32] and Dresselhaus [33] (β) constants of SOI, μ_B is the Bohr magneton, and g^* is an effective g-factor of the 2D system. For definiteness we assume α, β to be non-negative values and $\alpha \geqslant \beta$.

In the framework of the 2D model the Hamiltonian (1) does not depend on a component $P_z = p_z + eA_z/c$ of the generalized momentum and in the Coulomb gauge, $\mathbf{A} = (0, 0, B_x y - B_y x)$, $\nabla \cdot \mathbf{A} = 0$, can be rewritten as

$$\hat{H}_0 = \frac{\hbar^2(\hat{k}_x^2 + \hat{k}_y^2)}{2m}\sigma_0 + \alpha(\sigma_x\hat{k}_y - \sigma_y\hat{k}_x) + \beta(\sigma_x\hat{k}_x - \sigma_y\hat{k}_y) - \frac{g^*}{2}\mu_B(B_x\sigma_x + B_y\sigma_y), \quad (2)$$

where $\widehat{\mathbf{k}}$ is the wave-vector operator. Neglecting by cubic terms in the Dresselhaus part of Eqs. (1) and (2), we assume a narrow quantum well and small 2D wave vectors k of electrons in a conduction band, $k \ll \pi/w$, where w is the well width.

The eigenvalues and the eigenfunctions of the Hamiltonian (2) are (see, for example, Ref. [22])

$$\epsilon_{1,2}(\mathbf{k}) = \frac{\hbar^2 k^2}{2m} \pm \sqrt{(h_x + \alpha k_y + \beta k_x)^2 + (h_y - \alpha k_x - \beta k_y)^2}, \quad (3)$$

$$h_{x,y} = -\frac{g^*}{2}\mu_B B_{x,y},$$

$$\psi_{1,2}(\mathbf{r}) = \frac{1}{2\pi\sqrt{2}}e^{\mathbf{k}\cdot\mathbf{r}}\begin{pmatrix}1\\ \pm e^{i\theta}\end{pmatrix}. \quad (4)$$

The angle θ defines an average spin direction for two branches of the energy spectrum (3), $\theta = \theta_2 = \theta_1 + \pi$,

$$\tan\theta = \frac{h_y - \alpha k_x - \beta k_y}{h_x + \alpha k_y + \beta k_x}, \quad (5)$$

which depends on the wave vector and the magnetic field.

In the absence of magnetic field $h_x = h_y = 0$ the energy spectrum (3) is centrosymmetric $\epsilon_{1,2}(\mathbf{k}) = \epsilon_{1,2}(-\mathbf{k})$, and has two symmetry axes $k_x = k_y$ and $k_x = -k_y$. At $\alpha \neq \beta$ the energy branches $\epsilon = \epsilon_1(\mathbf{k})$ and $\epsilon = \epsilon_2(\mathbf{k})$ (energies as the function of the wave vector are three-dimensional surfaces in ϵ, k_x, k_y space) touch each other at the single point $\mathbf{k} = \mathbf{0}$, which is a conical (Dirac) point. In this point the energy of the ϵ_1 branch has the smallest value $\epsilon_1(0) = 0$. The energy branch $\epsilon = \epsilon_1(\mathbf{k}) \geqslant 0$ as a function of the wave-vector components k_x, k_y is a convex surface for any values of the parameters. The energy surface corresponding to the second branch $\epsilon = \epsilon_2(\mathbf{k})$ has two degenerate minima $\epsilon_2^{\min 1,2} = -\frac{m}{2\hbar^2}(\alpha + \beta)^2$ in the points $k_x^{\min 1,2} = k_y^{\min 1,2} = \mp\frac{m}{\sqrt{2}\hbar^2}(\alpha + \beta)$, two saddle points $k_x^{\text{sad}1,2} = -k_y^{\text{sad}1,2} = \pm\frac{m}{\sqrt{2}\hbar^2}(\alpha - \beta)$ corresponding to the energy $\epsilon_2^{\text{sad}1,2} = -\frac{m}{2\hbar^2}(\alpha - \beta)^2$, and a conical point $\epsilon_2(0) = 0$ at $\mathbf{k} = \mathbf{0}$.

The isoenergetic contours of constant energy $\epsilon_{1,2}(\mathbf{k}) = E$ (2D contours of a constant energy $\epsilon = E$ in the k_x, k_y plane) are a 2D analog of 3D Fermi surface pockets. At positive energies $E > 0$ the spectrum has two spin-split contours [see Fig. 1(b)]. The larger contour [$1(\epsilon_2)$, $2(\epsilon_2)$ in Fig. 1(b)] belongs to the branch $\epsilon = \epsilon_2$. The smaller contour [$1(\epsilon_1)$, $2(\epsilon_1)$ in Fig. 1(b)] of the branch $\epsilon = \epsilon_1$ is always situated inside the larger one. For $\epsilon_2(\mathbf{k}) = E < 0$ the isoenergetic contour becomes not simply connected: In the range $\epsilon_2^{\text{sad}1,2} < E < 0$ the contour of the smaller radius is situated inside the larger isoenergetic contour [contour 4 in the inset in Fig. 1(a)]. The electron velocity on this contour is directed along an inner normal, i.e., this contour can be interpreted as a "hole" one. At $E = \epsilon_2^{\text{sad}1,2}$ the contours become self-crossed. In the range $\epsilon_2^{\min 1,2} < E < \epsilon_2^{\text{sad}1,2}$ this contour splits into two parts which do not span the point $\mathbf{k} = \mathbf{0}$. The contours of the branch $\epsilon = \epsilon_2(\mathbf{k})$ are nonconvex in the energy interval [19]

$$\epsilon_2^{\text{sad}1,2} \leqslant E < -\frac{m(\alpha + \beta)^2(\alpha^2 - 6\alpha\beta + \beta^2)}{2\hbar^2(\alpha - \beta)^2}. \quad (6)$$

In the special case, $\alpha = \beta$, two energy spectrum branches contact along the parabola $\epsilon_1 = \epsilon_2 = \frac{\hbar^2 k^2}{2m}$ in the plane crossing the symmetry axis $k_x = -k_y$.

Plotting different dependencies in this paper, we use for numerical computations the dimensionless values

$$\bar{\alpha} = \frac{m\alpha}{\hbar^2 k_0}, \quad \bar{\beta} = \frac{m\beta}{\hbar^2 k_0}, \quad \bar{h} = \frac{h}{\epsilon_0}, \quad \bar{k} = \frac{k}{k_0}, \quad \bar{\epsilon} = \frac{\epsilon}{\epsilon_0}, \quad k_0 = \sqrt{2m\epsilon_0}/\hbar, \quad (7)$$

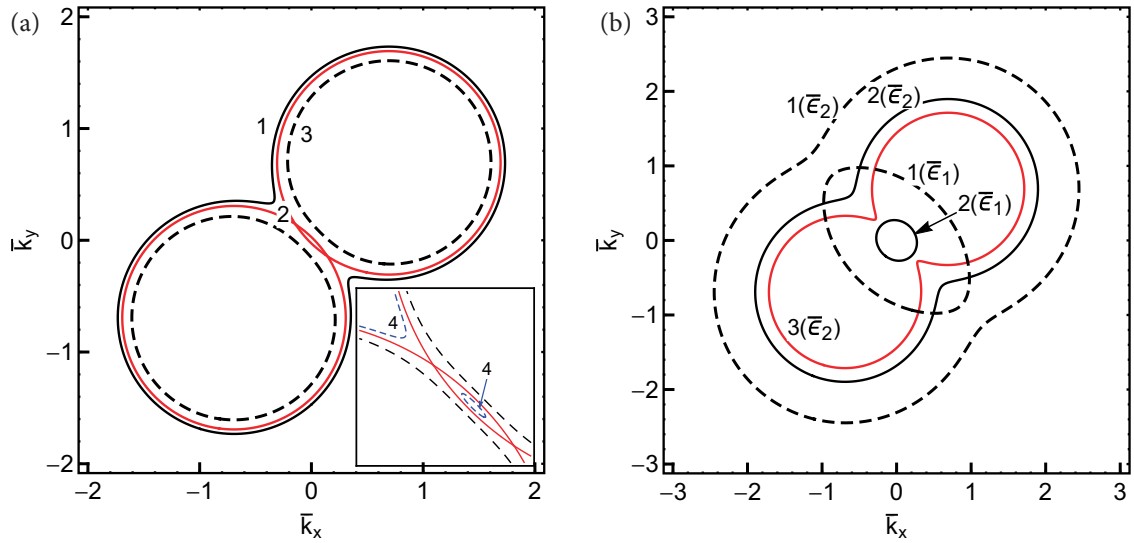

FIG. 1. Isoenergetic contours for different energies E at $h = 0$, $\bar{\epsilon}_2^{\min 1,2} = -0.72$, $\bar{\epsilon}_2^{\text{sad}1,2} = -0.02$, $\bar{\alpha} = 0.6$, $\bar{\beta} = 0.4$. (a) The contours belong to the branch $\epsilon = \epsilon_2$ at $E \leqslant 0$: $E = 0$, black solid contour (1); $\bar{E} = \bar{\epsilon}_2^{\text{sad}1,2} = -0.02$, red self-crossed contour (2); $\bar{E} = -0.1$, dashed contour (3). In the inset: $\bar{E} = -0.01$, blue short-dashed contour (4). (b) The contours $\epsilon_{1,2} = E$ at $E > 0$; $\bar{E} = 1$, dashed contours (1); $\bar{E} = 0.2$, black solid contours (2); $E = 0$, red solid contour (3).

where $\epsilon_0 > 0$ is a constant of energy dimension, for example, an absolute value of Fermi energy.

Figure 1 demonstrates the full set of Lifshitz transitions under changes of the energy: the appearance (or disappearance) of the new detached region at $E = 0$ [Fig. 1(b)], disruption (or formation) of the contour "neck" [Fig. 1(a)], and the appearance of the critical self-crossing contour at $\epsilon_2^{\text{sad}1,2} = E$ [contour 2 in Fig. 1(a)].

The concentration of 2D electron gas created in the heterostructures, and hence the Fermi energy, can be controlled by means of a gate electrode. Why is a magnetic field needed? In the system with a spin-orbit interaction an electric field perpendicular to the plane of 2D electrons not only shifts the Fermi level but also changes the Rashba SOI constant [34–36]. That may make the interpretation of experimental results ambiguous. A parallel magnetic field plays the role of an independent parameter which can tune the critical points of the energy spectrum to the Fermi energy. In the next sections we consider the possibility of driving the characteristics of the energy spectrum of 2D electron gas with RD SOI by means of an in-plane magnetic field.

III. ARBITRARY MAGNETIC FIELD DIRECTION: GENERAL RELATIONS

In a parallel magnetic field and $\alpha \neq \beta$ the point of the energy branch contact moves from the point $\mathbf{k} = \mathbf{0}$ to the point $\mathbf{k} = \mathbf{k}_0$ whose coordinates must be found from the condition

$$\sqrt{(h_x + \alpha k_{y0} + \beta k_{x0})^2 + (h_y - \alpha k_{x0} - \beta k_{y0})^2} = 0. \tag{8}$$

It is easy to see that Eq. (8) is equivalent to a system of linear inhomogeneous equations

$$\alpha k_{y0} + \beta k_{x0} = -h_x, \quad \alpha k_{x0} + \beta k_{y0} = h_y, \tag{9}$$

and we have

$$k_{x0} = h\frac{\alpha \sin\varphi_h + \beta \cos\varphi_h}{\alpha^2 - \beta^2},$$
$$k_{y0} = -h\frac{\alpha \cos\varphi_h + \beta \sin\varphi_h}{\alpha^2 - \beta^2}, \tag{10}$$

where angle φ_h defines the magnetic field direction $\mathbf{h} = h(\cos\varphi_h, \sin\varphi_h, 0)$. The energy value corresponding to the point $\mathbf{k} = \mathbf{k}_0 = (k_{x0}, k_{y0})$ (10) is given by

$$\epsilon_1(\mathbf{k}_0) = \epsilon_2(\mathbf{k}_0) = E_0 = h^2\hbar^2\frac{\alpha^2 + \beta^2 + 2\alpha\beta \sin 2\varphi_h}{2m(\alpha^2 - \beta^2)^2}. \tag{11}$$

If the SOI constants are equal, $\alpha = \beta$, Eqs. (9) have nonzero solutions only if $h_x = -h_y$. In this case the branches contact along the parabola

$$\epsilon_{\text{cont}}(k_{y1}, h) = \frac{\hbar^2 k_{y1}^2}{2m} + \frac{\hbar^2 h^2}{8m\alpha^2},$$
$$k_{x1} = \frac{k_x + k_y}{\sqrt{2}} = \frac{h}{2\alpha}, \tag{12}$$
$$k_{y1} = \frac{k_x - k_y}{\sqrt{2}}.$$

For any other directions of the vector $\mathbf{h}$ the branches do not have common points for $\alpha = \beta$.

For a further analysis of the energy spectrum at $\alpha \neq \beta$ it is useful to introduce polar coordinates $\tilde{k} > 0$, and f with the center in the point $\mathbf{k}_0$ (10),

$$k_x = k_{x0} + \tilde{k}\cos f, \quad k_y = k_{y0} + \tilde{k}\sin f. \tag{13}$$

Note that new coordinates only shift the energy spectrum in $\mathbf{k}$ space and they do not change the differential characteristics of $\epsilon = \epsilon_{1,2}(\mathbf{k})$ surfaces.

In coordinates $\tilde{k}, f$ (13) the energies $\epsilon_{1,2}$ take the simple form

$$\epsilon_{1,2}(\tilde{k}, \tilde{f}) = \frac{\hbar^2\tilde{k}^2}{2m} - \frac{\hbar^2\tilde{k}}{m}\lambda_{1,2}(f) + E_0, \tag{14}$$

where

$$\lambda^{(1,2)}(f) = h\frac{\alpha\sin(f-\varphi_h) - \beta\cos(f+\varphi_h)}{\alpha^2-\beta^2} \mp \frac{m}{\hbar^2}\sqrt{\alpha^2+\beta^2+2\alpha\beta\sin(2f)}, \tag{15}$$

$$\lambda^{(2)}(f) = -\lambda^{(1)}(f+\pi). \tag{16}$$

Substituting Eqs. (13) into formula (5), one finds that spin directions are antisymmetric, $\theta(f+\pi) = \theta(f) + \pi$, with respect to the point $\mathbf{k}_0 = (k_{x0}, k_{y0})$.

The sign of the Gaussian curvature $K^{(1,2)}(\tilde{k}, f)$ of energy surfaces $\epsilon = \epsilon_{1,2}(\tilde{k}, \tilde{f})$ is defined by the sign of the determinant $\det(H)$ of the Hessian matrix,

$$H = \begin{pmatrix} \frac{\partial^2\epsilon_{1,2}}{\partial k_x^2} & \frac{\partial^2\epsilon_{1,2}}{\partial k_x\partial k_y} \\ \frac{\partial^2\epsilon_{1,2}}{\partial k_y\partial k_x} & \frac{\partial^2\epsilon_{1,2}}{\partial k_y^2} \end{pmatrix}. \tag{17}$$

In coordinates (13) one finds

$$\det(H) = \frac{\hbar^4}{m^2\tilde{k}}[\tilde{k} - \ddot{\lambda}^{(1,2)}(f) - \lambda^{(1,2)}(f)]. \tag{18}$$

Here and in all formulas below the points above the functions denote the derivative with respect to the angle f. From Eq. (15) one can see that the sum of $\lambda^{(1,2)}$ and its second derivatives $\ddot{\lambda}^{(1,2)}$ do not depend on magnetic field and have the definite sign

$$\ddot{\lambda}^{(1,2)}(f) + \lambda^{(1,2)}(f) = \mp\frac{m}{\hbar^2}\frac{(\alpha^2-\beta^2)^2}{[\alpha^2+2\alpha\beta\sin(2f)+\beta^2]^{3/2}}. \tag{19}$$

From Eqs. (18) and (19) it follows that $K^{(1)}(\tilde{k}, f) > 0$ for any values of the parameters, i.e., the surface $\epsilon = \epsilon_1(\tilde{k}, \tilde{f})$ is the convex one.

Critical points $(\tilde{k}_\nu, f_\nu)$ of the energy spectrum should be found from the system of equations

$$\frac{\partial\epsilon_{1,2}}{\partial\tilde{k}} = \frac{\hbar^2}{m}[\tilde{k} - \lambda^{(1,2)}(f)] = 0, \quad \tilde{k} \geqslant 0, \tag{20}$$

$$\frac{\partial\epsilon_{1,2}}{\partial f} = -\frac{\hbar^2}{m}\tilde{k}\dot{\lambda}^{(1,2)}(f) = 0, \tag{21}$$

from which we give

$$\tilde{k}_\nu^{(1,2)} = \lambda^{(1,2)}\big(f_\nu^{(1,2)}\big), \tag{22a}$$

$$\dot{\lambda}^{(1,2)}\big(f_\nu^{(1,2)}\big) = 0, \tag{22b}$$

where index ν numerates the roots of Eq. (21). According to the definition, the variable $\tilde{k}$ is an absolute value of the electron wave vector in coordinates (13). Only the solutions for which $\tilde{k}_\nu^{(1,2)} = \lambda^{(1,2)}(f_\nu^{(1,2)}) > 0$ have a physical meaning.

The obvious equality (16) gives the relations between solutions (22),

$$f_\nu^{(1)} = f_\nu^{(2)} + \pi, \quad \tilde{k}\big(f_\nu^{(1)}\big) = -\tilde{k}\big(f_\nu^{(2)}\big), \quad \ddot{\lambda}^{(1)}\big(f_\nu^{(1)}\big) = -\ddot{\lambda}^{(2)}\big(f_\nu^{(2)}\big). \tag{23}$$

The determinant $\det(H)$ (18) in the critical points reads

$$\det[H(\tilde{k}_\nu, f_\nu)] = -\frac{\hbar^4}{m^2\tilde{k}}\ddot{\lambda}^{(1,2)}(f)\Big|_{\tilde{k}=\tilde{k}_\nu, f=f_\nu^{(1,2)}}, \quad \tilde{k} > 0. \tag{24}$$

If $\ddot{\lambda}^{(1,2)} \neq 0$, the critical point is nondegenerate. From Eq. (24) we conclude that the negative second derivative $\ddot{\lambda}^{(1,2)}(f_\nu^{(1,2)}) < 0$ corresponds to energy minima $\epsilon_{1,2}(\tilde{k}_\nu, f_\nu^{(1,2)}) = \epsilon_{1,2}^{\min}$ and for saddle points of the nonconvex surface $\epsilon_2(\tilde{k}_\nu, f_\nu^{(1,2)}) = \epsilon_2^{\rm sad}$ the second derivative is positive, $\ddot{\lambda}^{(2)}(f_\nu^{(1,2)}) > 0$. As it easy to see from Eqs. (14) and (22), the energies in the critical points are written as

$$\epsilon_{1,2}^{\rm crit} = \epsilon_{1,2}\big(\tilde{k}_\nu, f_\nu^{(1,2)}\big) = E_0 - \frac{\hbar^2}{2m}\big[\lambda^{(1,2)}\big(f_\nu^{(1,2)}\big)\big]^2, \tag{25}$$

i.e., all the critical points are situated below the energy level $E = E_0$. So, the evolution of either energy branch of 2D electrons with RD SOI under the influence of a parallel magnetic field is completely described by means of the single function $\lambda^{(1,2)}(f)$ (15).

For an arbitrary magnetic field Eq. (22b) can be transformed to a quartic equation for $\cos(2f_\nu^{(1,2)})$, the exact solutions of which are well known. Unfortunately they are so lengthy that they are not suitable for any analytical calculation. Nevertheless, for numerical computations the solution of Eq. (22b) presents no problems.

The limiting cases of weak and strong magnetic fields can be analyzed by means of the expansions of the exact eigenenergies (3). For the weak magnetic field the power expansion of energy ϵ_2 (3) on h gives energies of the critical points and their positions. As a result of the direct calculations, one obtains the following expressions for two minima,

$$\epsilon_2^{\min\,1,2} \simeq -\frac{m}{2\hbar^2}(\alpha+\beta)^2 \mp h\sin\left(\varphi_h - \frac{\pi}{4}\right), \quad h \ll \frac{m}{\hbar^2}(\alpha+\beta)^2, \tag{26}$$

$$k_x^{\min\,1,2} = k_y^{\min\,1,2} \simeq \mp\frac{m}{\hbar^2}\frac{\alpha+\beta}{\sqrt{2}} - \frac{(\alpha-\beta)h\sin\left(\varphi_h+\frac{\pi}{4}\right)}{\sqrt{2}(\alpha+\beta)^2}, \tag{27}$$

and two saddle points,

$$\epsilon_2^{\rm sad1,2} \simeq -\frac{m}{2\hbar^2}(\alpha-\beta)^2 \pm h\sin\left(\varphi_h + \frac{\pi}{4}\right), \quad h \ll \frac{m}{\hbar^2}(\alpha-\beta)^2, \tag{28}$$

$$k_x^{\rm sad1,2} = -k_y^{\rm sad1,2} \simeq \pm\frac{\alpha-\beta}{\sqrt{2}}\frac{m}{\hbar^2} - \frac{h(\alpha+\beta)\sin\left(\varphi_h-\frac{\pi}{4}\right)}{\sqrt{2}(\alpha-\beta)^2}. \tag{29}$$

The branch ϵ_1 in this case does not have an extremum. The energy ϵ_1 reaches the least value $\epsilon_1(\mathbf{k}_0) = E_0$ (11) in the point of the branch contact $\mathbf{k}_0 = (k_{x0}, k_{y0})$ (10).

In the strong magnetic field $h \gg \frac{m}{\hbar^2}(\alpha^2 + \beta^2 - 2\alpha\beta \sin 2\varphi_h)$ the power series of $\epsilon_{1,2}$ (3) on $1/h$ gives the energy minima $\epsilon_{1,2}^{\min}$ of both branches,

$$\epsilon_{1,2}^{\min} \simeq \pm h - \frac{m}{2\hbar^2}(\alpha^2 + \beta^2 - 2\alpha\beta \sin 2\varphi_h), \tag{30}$$

$$k_{x1,2}^{\min} \simeq \pm\frac{m}{\hbar^2}(\alpha \sin\varphi_h - \beta\cos\varphi_h),$$

$$k_{y1,2}^{\min} \simeq \pm\frac{m}{\hbar^2}(\beta \sin\varphi_h - \alpha\cos\varphi_h). \tag{31}$$

So, with increasing magnetic field, the energy spectrum evolves from the energy branch ϵ_2 having four critical points and the branch ϵ_1 without critical points to the spectrum whose every branch has a single critical (minimum) point. How does such an evolution occur? For an arbitrary magnetic field direction some general conclusions can be made on the basis of the properties of functions $\lambda^{(1,2)}(f)$ (15) and its derivatives $\dot{\lambda}^{(1,2)}(f)$, $\ddot{\lambda}^{(1,2)}(f)$.

As it has been concluded above, the branch $\epsilon = \epsilon_1$ is convex and does not have saddle points. It is clear from Eq. (15) at a weak magnetic field ($h \to 0$) $\lambda^{(1)}(f) < 0$ for any angle f, i.e., for the energy branch $\epsilon = \epsilon_1(\mathbf{k})$ Eq. (20) does not have positive solutions $\tilde{k} > 0$. The critical value $h = h_{c2}$ can be derived by means of the equation $\lambda^{(1)}(h = h_{c2}; f) = 0$ from which we find

$$h_{c2} = \frac{m}{\hbar^2}\frac{(\alpha^2 - \beta^2)^2}{\sqrt{\alpha^4 + 6\alpha^2\beta^2 + \beta^4 + 4\alpha\beta(\alpha^2 + \beta^2)\sin 2\varphi_h}}. \tag{32}$$

Substituting $\lambda^{(1)}(f)$ (15) in Eq. (25) and taking into account the positiveness of the function $\lambda^{(1)}(f_\nu^{(1)}) > 0$ at $h > h_{c2}$, it is easy to show that $0 \leqslant \epsilon_1^{\min} \leqslant E_0$ for any values of the parameters. As it follows from Eq. (23), the appearance of minima of the branch ϵ_1 is accompanied by the disappearance of the saddle point of the branch ϵ_2.

The energy surface $\epsilon = \epsilon_2$ has regions of negative Gaussian curvature. The derivative $\dot{\lambda}^{(2)}(f)$ is the sum of the oscillatory functions with periods 2π and π. Depending on the magnetic field value it has two zeros at $h > h_{c1}$ and four zeros at $h < h_{c1}$ in the range $[-\pi, \pi]$. The numbers of zeros $\dot{\lambda}^{(2)}(f)$ having a different sign of the second derivative $\ddot{\lambda}^{(2)}(f)$ are equal. The critical value h_{c1} can be found from the condition of the coalescence of two zeros of $\dot{\lambda}^{(2)}(h, f)$ with different signs of the second derivative $\ddot{\lambda}^{(2)}(h; f)$ which at this point vanishes, i.e., one should search two unknown quantities h_{c1}, f_c from the two equations

$$\dot{\lambda}^{(2)}(h_{c1}, f_c) = 0, \quad \ddot{\lambda}^{(2)}(h_{c1}, f_c) = 0. \tag{33}$$

We could not find the analytical solution of this system for an arbitrary magnetic field orientation. The critical fields h_{c1} in an explicit form for special directions of vector $\mathbf{h}$ are found in the next section. Note that the sign of the difference $h_{c2} - h_{c1}$ is not fixed for a given α, β and depends on the magnetic field direction.

The evolution of the branch $\epsilon = \epsilon_2(\mathbf{k})$ can be understood from Fig. 2. In the magnetic field $h < \min(h_{c1}, h_{c2})$, $\tilde{k}_\nu^{(2)} = \lambda^{(2)}(f_\nu^{(2)}) > 0$, and there are four critical points $\dot{\lambda}^{(2)}(f_\nu^{(2)}) = 0$—two minima $\epsilon_2^{\min 1,2}$ [$\ddot{\lambda}^{(1,2)}(f_\nu) < 0$] and two saddle points $\epsilon_2^{\text{sad}1,2}$ [$\ddot{\lambda}^{(1,2)}(f_\nu) > 0$] [Fig. 2(a)]. At $h = h_{c2}$ one of the saddle points coincides with the point of branch contact, $\tilde{k}_\nu^{(2)} = \lambda^{(2)}(f_\nu^{(2)}) = 0$, and "disappears" [Fig. 2(b)]. In the magnetic field $h = h_{c1}$ the minimum and saddle points of the energy surface $\epsilon = \epsilon_2$ "annihilate" [Fig. 2(c)] and in larger fields $h > \max(h_{c1}, h_{c2})$ the branch $\epsilon = \epsilon_2(\mathbf{k})$ has one absolute minimum [Fig. 2(d)].

Below, we consider some cases when the exact formulas become elementary and give clear illustrations of the general conclusion of this section.

IV. MAGNETIC FIELD ALONG THE SYMMETRY AXIS

For the direction of the magnetic field along one of the symmetry axes the energy spectrum preserves the symmetry with respect to the other axis. This circumstance essentially simplifies the solution of the equations obtained above.

A. Magnetic field directed along the $k_x = -k_y$ axis

Let us consider the magnetic field direction $\varphi_h = 3\pi/4$. In this case, Eq. (21), from which the angles f_ν ($\nu = 1, 2, 3, 4$) corresponding to zeros of derivative $\lambda_{1,2}$, can be found. Equation (22b) has four solutions in the interval $[-\pi, \pi]$. Two solutions do not depend on the magnetic field and SOI constants,

$$f_1^{(1,2)} = -\frac{3\pi}{4}, \quad f_2^{(1,2)} = \frac{\pi}{4}, \tag{34}$$

and two solutions exist in the finite interval of value $h \in [0, h_{c1}]$,

$$f_3^{(1,2)}(h) = -\frac{\pi}{4} \mp \arcsin(\eta),$$

$$f_4^{(1,2)}(h) = \frac{3\pi}{4} \pm \arcsin(\eta), \tag{35}$$

where

$$\eta(\alpha, \beta, h) = \frac{h(\alpha - \beta)}{2\sqrt{\alpha\beta(h_{c1}h_{c2} - h^2)}},$$

$$\eta \leqslant 1 \Leftrightarrow h \leqslant h_{c1}. \tag{36}$$

The functions $\lambda^{(2)}(f_\nu^{(1,2)})$ and $\ddot{\lambda}^{(2)}(f_\nu^{(1,2)})$ which define the energy of the critical points and their character are presented in the Appendix. The critical magnetic fields in the case under consideration are

$$h_{c1} = \frac{4m}{\hbar^2}\alpha\beta, \quad h_{c2} = \frac{m}{\hbar^2}(\alpha + \beta)^2. \tag{37}$$

In accordance with Eqs. (25) and (A1) for any value of magnetic field the energy of the branch $\epsilon = \epsilon_2$ has a minimum $\epsilon_2^{\min 1}$,

$$\epsilon_2^{\min 1}(h) = \epsilon^{\text{crit}1}(h), \quad f_1^{(2)} = -\frac{3\pi}{4},$$

$$\tilde{k}_1^{(2)}(h) = \frac{m}{\hbar^2}(\alpha + \beta) + \frac{h}{\alpha + \beta}. \tag{38}$$

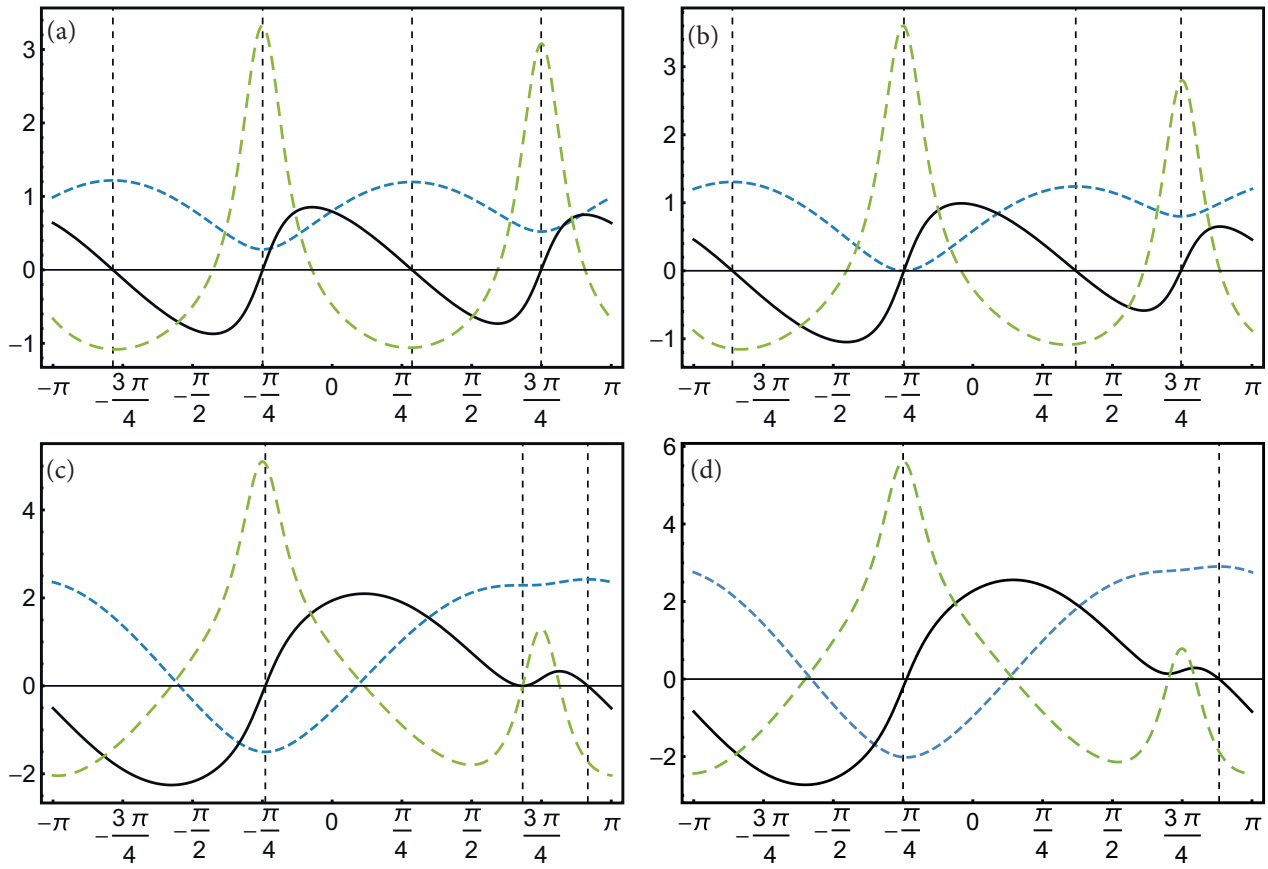

FIG. 2. The dependencies of the function $\lambda_2(f)$ (15) (short dashed lines), its first $\dot{\lambda}_2(f)$ (solid lines) and second $\ddot{\lambda}_2(f)$ (long dashed lines) derivatives on the angle $f \in [-\pi, \pi]$ for different values of magnetic field h: (a) $\bar{h} = 0.05 < \bar{h}_{c2} = 0.1655$; (b) $h = h_{c2}$; (c) $\bar{h} = \bar{h}_{c1} = 0.7867$; (d) $\bar{h} = 1 > \bar{h}_{c1}$. Vertical dashed lines show angles $f = f_v^{(2)}$ corresponding to $\dot{\lambda}_2(f_v^{(2)}) = 0$. For SOI constants and magnetic field direction we used the values $\bar{\alpha} = 0.8$, $\bar{\beta} = 0.4$, $\varphi_h = \pi/3$.

With an increase in magnetic field the minimum $\epsilon_2^{\min 1}$ moves down. The second minimum of this branch $\epsilon_2^{\min 2}$,

$$\epsilon_2^{\min 2}(h) = \epsilon^{\mathrm{crit2}}(h), \quad f_2^{(2)} = \frac{\pi}{4},$$
$$\tilde{k}_2^{(2)}(h) = \frac{m}{\hbar^2}(\alpha+\beta) - \frac{h}{\alpha+\beta}, \tag{39}$$

exists in the field interval $0 \leqslant h < h_{c1}$. In this interval the branch ϵ_2 has two saddle points with equal energies,

$$\epsilon_2^{\mathrm{sad3,4}}(h) = \epsilon^{\mathrm{crit3,4}}(h), \quad f = f_{3,4}^{(2)},$$
$$\tilde{k}_{3,4}^{(2)}(h) = \frac{m}{h^2}(\alpha-\beta)\sqrt{1-\frac{h^2}{h_{c1}h_{c2}}}. \tag{40}$$

In the field $h \to h_{c1}$ the minimum $\epsilon_2^{\min 2}$ transforms to the saddle point $\epsilon_2^{\min 2} \to \epsilon_2^{\mathrm{sad}} = \epsilon^{\mathrm{crit2}}$ [the second derivative $\ddot{\lambda}^{(2)}$ (A4) changes sign at $h = h_{c1}$] which blends with two saddle points $\epsilon_2^{\mathrm{sad3,4}}$ (40), i.e., the critical point becomes degenerate,

$$\epsilon^{\min 2}(h_{c1}) = \epsilon_2^{\mathrm{sad}}(h_{c1}) = \epsilon_2^{\mathrm{sad3,4}}(h_{c1}) = -\frac{m}{2\hbar^2}(\alpha^2 - 6\alpha\beta + \beta^2),$$
$$\tilde{k}_2^{(2)}(h_{c1}) = \tilde{k}_{3,4}^{(2)}(h_{c1}) = \frac{m(\alpha-\beta)^2}{\hbar^2(\alpha+\beta)},$$
$$f_2^{(2)}(h_{c1}) = f_{3,4}^{(2)}(h_{c1}) = \frac{\pi}{4}. \tag{41}$$

In larger fields $h_{c1} < h < h_{c2}$ the saddle point $\epsilon_2^{\mathrm{sad}}$ exists. At $h \to h_{c2}$ its energy $\epsilon_2^{\mathrm{sad}} \to E_0$ and this saddle point disappears in the field $h = h_{c2}$ [$\dot{\lambda}^{(2)}$ (A1) becomes negative at $h > h_{c2}$],

$$\epsilon^{\mathrm{crit2}}(h_{c2}) = \epsilon_2^{\mathrm{sad}}(h_{c2}) = E_0(h_{c2}) = \frac{m}{2\hbar^2}(\alpha+\beta)^2,$$
$$\tilde{k}_2^{(2)}(h_{c2}) = 0, \quad f_2^{(2)} = \frac{\pi}{4}. \tag{42}$$

In the magnetic fields $h > h_{c2}$ the function $\lambda^{(1)}(\pi/4)$ (A1) becomes positive and the first energy branch ϵ_1 acquires the critical point (minimum) $\epsilon_1^{\min} = \epsilon^{\mathrm{crit2}}$,

$$\epsilon_1^{\min}(h) = \epsilon^{\mathrm{crit2}}, \quad f_2^{(1)} = \frac{\pi}{4},$$
$$\tilde{k}_2^{(1)} = -\frac{m}{\hbar^2}(\alpha+\beta) + \frac{h}{\alpha+\beta}. \tag{43}$$

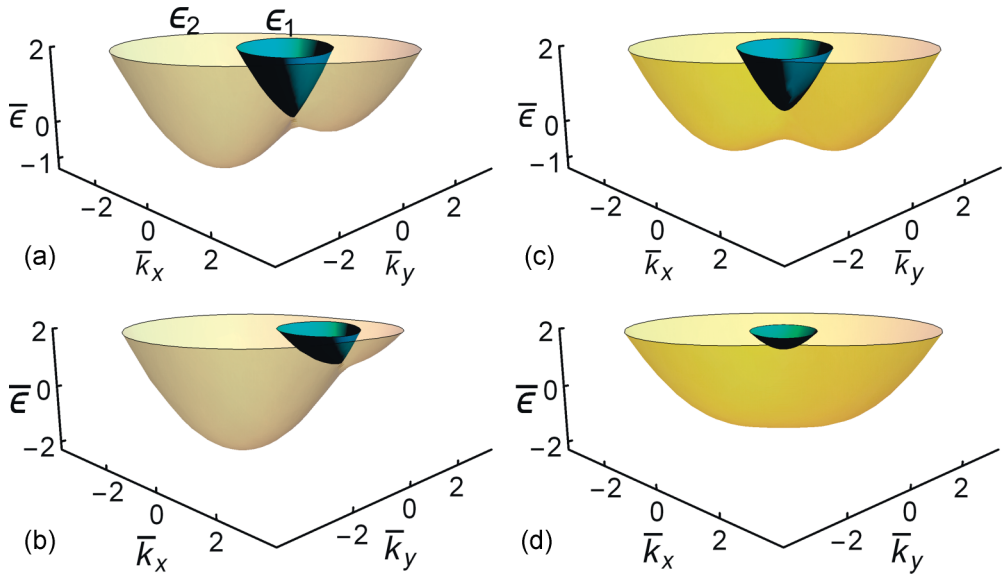

FIG. 3. Energy spectrum (3) for the magnetic field directed (a), (b) along the $k_x = -k_y$ axis, $\varphi_h = 3\pi/4$, and (c), (d) along the $k_x = k_y$ axis. (a), (c) $\bar{h} = 0.5 < \bar{h}_{c1} = 1.28$, $\bar{h}_{c2} = 1.44$; (b), (d) $\bar{h} = 1.5 > \bar{h}_{c1}, \bar{h}_{c2}$. For SOI constants we used the values $\bar{\alpha} = 0.8$, $\bar{\beta} = 0.4$.

The minimum $\epsilon_1^{\min}$ moves up with an increase in the magnetic field. The discussed evolution of the energy spectrum is illustrated in Fig. 3.

B. Magnetic field directed along the $k_x = k_y$ axis

In this case the solutions of Eq. (22b) take the form (we choose $\varphi_h = \pi/4$)

$$\begin{aligned} f_1^{(1,2)} &= \frac{3\pi}{4}, \quad f_2^{(1,2)} = -\frac{\pi}{4}, \\ f_3^{(1,2)}(h) &= \frac{\pi}{4} \mp \arcsin(\eta), \\ f_4^{(1,2)}(h) &= \frac{5\pi}{4} \pm \arcsin(\eta), \end{aligned} \tag{44}$$

where

$$\begin{aligned} \eta(\alpha, \beta, h) &= \frac{h(\alpha+\beta)}{2\sqrt{\alpha\beta(h_{c1}h_{c2}+h^2)}}, \\ \eta \leqslant 1 &\Leftrightarrow h \leqslant h_{c1}. \end{aligned} \tag{45}$$

The critical magnetic fields are

$$h_{c1} = \frac{4m}{\hbar^2}\alpha\beta, \quad h_{c2} = \frac{m}{\hbar^2}(\alpha-\beta)^2. \tag{46}$$

As it follows from formulas (A9)–(A14) in the Appendix, at $h < h_{c2}$ the branch $\epsilon = \epsilon_2$ has two minima $\epsilon_2^{\min 1,2}$ with equal energies,

$$\begin{aligned} \epsilon_2^{\min 1,2}(h) &= -\frac{m}{2\hbar^2}(\alpha+\beta)^2 - \frac{h^2\hbar^2}{8m\alpha\beta}, \quad h \leqslant h_{c1}, \\ k_{3,4}^{(2)} &= \frac{m}{\hbar^2}(\alpha+\beta)\sqrt{1+\frac{h^2}{h_{c1}h_{c2}}}, \quad f = f_{3,4}^{(2)}, \end{aligned} \tag{47}$$

and two saddle points $\epsilon_2^{\text{sad}1,2}$ [see Fig. 3(a)],

$$\begin{aligned} \epsilon_2^{\text{sad}1,2}(h) &= -\frac{m}{2\hbar^2}(\alpha-\beta)^2 \mp h, \\ \tilde{k}_{1,2}^{(2)}\big(f_{1,2}^{(2)}\big) &= \frac{m}{\hbar^2}(\alpha-\beta) \mp \frac{h}{\alpha-\beta}, \\ f_1^{(2)} &= -\frac{\pi}{4}, \quad f_2^{(2)} = \frac{3\pi}{4}. \end{aligned} \tag{48}$$

In the magnetic field $h = h_{c1}$ both minima $\epsilon_2^{\min 1,2}$ and the saddle point $\epsilon_2^{\text{sad}1}$ transform into one degenerate critical point,

$$\epsilon_2^{\min 1,2}(h_{c1}) = \epsilon_2^{\text{sad}2}(h_{c1}) = -\frac{m}{2\hbar^2}(\alpha^2+6\alpha\beta+\beta^2), \tag{49}$$

$$f_3^{(4)}(h_{c1}) = f_4^{(2)}(h_{c1}) = f_2^{(2)} = \frac{3\pi}{4}, \tag{50}$$

$$\begin{aligned} \widetilde{k}_2^{(2)}(h_{c1}) = \widetilde{k}_{3,4}^{(2)}(h_{c1}) &= \frac{m}{\hbar^2}\frac{(\alpha+\beta)^2}{\alpha-\beta}, \\ \ddot{\lambda}^{(2)}\left(h_{c1}, \frac{3\pi}{4}\right) = \ddot{\lambda}^{(2)}\big(h_{c1}, f_{3,4}^{(2)}\big) &= 0, \end{aligned} \tag{51}$$

and for larger fields $h > h_{c1}$ one minimum,

$$\begin{aligned} \epsilon_2^{\min}(h) &= -\frac{m}{2\hbar^2}(\alpha-\beta)^2 - h, \\ \tilde{k}_1^{(2)}\big(f_1^{(2)}\big) &= \frac{m}{\hbar^2}(\alpha-\beta) - \frac{h}{\alpha-\beta}, \quad f_1^{(2)} = -\frac{\pi}{4}, \end{aligned} \tag{52}$$

and one saddle point remains,

$$\begin{aligned} \epsilon_2^{\text{sad}}(h) &= -\frac{m}{2\hbar^2}(\alpha-\beta)^2 + h, \\ \tilde{k}_2^{(2)}\big(f_2^{(2)}\big) &= \frac{m}{\hbar^2}(\alpha-\beta) + \frac{h}{\alpha-\beta}, \quad f_2^{(2)} = \frac{3\pi}{4}, \end{aligned} \tag{53}$$

which exists until $h < h_{c2}$.

The first branch $\epsilon = \epsilon_1$ reaches the smallest value,

$$E_0 = \frac{h^2\hbar^2}{2m(\alpha-\beta)^2}, \tag{54}$$

at the weak magnetic field $h < h_{c2}$. If $h > h_{c2}$, this branch has the minimum [see Fig. 3(b)]

$$\epsilon_1^{\min}(h) = -\frac{m}{2\hbar^2}(\alpha-\beta)^2 + h, \tag{55}$$

$$\tilde{k}_1^{(1)} = -\frac{m}{\hbar^2}(\alpha-\beta) + \frac{h}{\alpha-\beta}, \quad f_1^{(1)} = \frac{3\pi}{4}. \tag{56}$$

The results of this section and Fig. 3 illustrate a quite different evolution of the energy spectrum for the same values of SOI constants but different magnetic field directions.

V. ISOENERGETIC CONTOURS

The dispersion relation of 2D electron gas can be characterized by isoenergetic contours $\epsilon_{1,2} = E = \text{const}$. According to the theory of electron topological transitions [2,3], when the energy level E crosses the energy of the critical point $\epsilon_{1,2}^{\text{crit}}$, the isoenergetic contours change their topology. By analogy with the 3D case we name the 2D contours at $E = \epsilon_{1,2}^{\text{crit}}$ as critical contours. The critical contours always have the point $(\tilde{k}_v, f_v)$ (22b) in which the electron velocity $\mathbf{v} = \frac{\partial\epsilon_{1,2}}{\hbar\partial\mathbf{k}} = \mathbf{0}$,

$$|\mathbf{v}| = \sqrt{\left(\frac{\partial\epsilon_{1,2}}{\hbar\partial k_x}\right)^2 + \left(\frac{\partial\epsilon_{1,2}}{\hbar\partial k_y}\right)^2} = \frac{\hbar}{m}\sqrt{[\tilde{k} - \lambda^{(1,2)}(f)]^2 + [\dot{\lambda}^{(1,2)}(f)]^2}]. \tag{57}$$

In this regard a self-crossing contour is not a critical one because $\mathbf{v} \neq \mathbf{0}$ at the cross point. However, one should remember that the cross point is a particular point in a vicinity of which the electron dispersion is linear in the wave-vector components. For the minimum point $\epsilon_{1,2}^{\text{crit}} = \epsilon_{1,2}^{\min}$ the contour is absent for energy $E < \epsilon_{1,2}^{\min}$, while for saddle points $\epsilon_2^{\text{crit}} = \epsilon_2^{\text{sad}}$ the contours exist both at $E < \epsilon_2^{\text{sad}}$ and $E > \epsilon_2^{\text{sad}}$.

The positive roots of the equation [see Eq. (14)]

$$\epsilon_{1,2}(\tilde{k}, f) = \frac{\hbar^2\tilde{k}^2}{2m} - \frac{\hbar^2\tilde{k}}{m}\lambda_{1,2}(f) + E_0 = E \tag{58}$$

describe the isoenergetic contours $k = k_\pm^{(j)}(E, f)$ corresponding to physical electron states in $\mathbf{k}$ space for a given energy E,

$$k_\pm^{(1,2)} = \lambda^{(1,2)} \pm \sqrt{\xi^{(1,2)}}, \tag{59}$$

$$\xi^{(1,2)} = (\lambda^{(1,2)})^2 + \frac{2m(E-E_0)}{\hbar^2} \geqslant 0. \tag{60}$$

If $E > E_0$, the roots $k_+^{(1,2)} > 0$ for any values of f, while roots $k_-^{(1,2)} < 0$, i.e., there are two contours belonging to different energy branches. For $E < E_0$ the real roots of Eq. (58) exist, if the inequality $2m(E_0 - E)/\hbar^2 \leqslant (\lambda^{(1,2)})^2$ holds. Roots $k_\pm^{(1,2)}$ take positive values for the angles f at which $\lambda^{(1,2)} > 0$. This means that the wave vector crosses the isoenergetic contour twice.

In accordance with Vieta's formulas, the roots of Eq. (58) obey the relations

$$k_+^{(1,2)}k_-^{(1,2)} = \frac{2m(E_0-E)}{\hbar^2}, \quad k_+^{(1,2)} + k_-^{(1,2)} = 2\lambda^{(1,2)}, \tag{61}$$

from which an interesting observation follows: At $E = E_0$ the extremal radii of the contours $k_+^{(1,2)} = 2\lambda^{(1,2)}$, for which $\dot{\lambda}^{(1,2)} = 0$, give energies (25) and positions (22) of the critical points on the total surfaces $\epsilon = \epsilon_{1,2}$.

From the properties of the energy spectrum which have been discussed in Sec. III, some general conclusions related to the isoenergetic contours follow: (1) There are one or two separate contours for a given energy E. (2) The contours belonging to the branch $\epsilon = \epsilon_1$ exist for the energies $E > E_0$ at $h < h_{c2}$ and $E > \epsilon_1^{\min}$ at $h > h_{c2}$. Contours $k = k_\pm^{(1)}(f)$ are convex by virtue of the equality (19). (3) In magnetic fields $h > h_{c1}$ the contour on the surface $\epsilon = \epsilon_2$ splits into two separated contours for $E < \min(\epsilon_2^{\text{sad}1,2})$.

At fixed energy E the magnetic field moves the energy of the branch contact E_0 (11) and the energies of the critical points (25), resulting in a Lifshitz electron transition of both types—the appearance of a new contour under crossing the energy E by minimum $\epsilon_{1,2}^{\min}$ and disruption of the "neck" at $E = \epsilon_2^{\text{sad}}$.

At equal SOI constants $\alpha = \beta$ and the magnetic field direction along the axis $k_x = -k_y$ for energies $E > \hbar^2h^2/8m\alpha^2$, the isoenergetic contours have two common contact points. Either contour consists of two arcs of the radius (see Fig. 7),

$$k^{(\pm)} = \sqrt{\frac{2m}{\hbar^2}\left(E + \frac{2m\alpha^2}{\hbar^2} \mp h\right)}. \tag{62}$$

The spin directions on each arc composing a united contour are opposite, $\theta_+ = 3\pi/4$ or $\theta_- = -\pi/4$, and the arcs, which have the same spin direction $\theta_\pm$, form the total circumference.

Figures 4 and 5 illustrate some of the explicit results obtained in Sec. IV A for the magnetic field directed along the axis $k_x = -k_y$. Figure 4(a) shows the changes in the fine structure of the isoenergetic contours of the branch $\epsilon = \epsilon_2$ for the energy close to the energy of the saddle point $\epsilon_2^{\text{sad}3,4}(h)$ (40) at magnetic fields far from the critical values $h < h_{c1}, h_{c2}$ (37). In this case we observe a specific topological transition of the contour splitting in the transverse to the "neck" direction. With the increase in the magnetic field the electron and "hole" contours (curves 1) form a unified critical contour with two crossing points (curve 2). The critical contour breaks at the crossing points in the transverse direction forming two electron contours (curves 3). Figure 4(b) shows the disruption of the neck in the case when the energy $E < E_0(h_{c1})$ equals the energy of the saddle point $E = \epsilon_2^{\text{sad}3,4}(h_{c1})$ (40) at the critical field h_{c1} (37). Two separate contours (curves 1) touch at $h = h_{c1}$ and in a higher field form a single nonconvex contour (curves 3 and 4).

Figure 5 illustrates another type of topological transition in the magnetic field: the disappearance (or appearance) of a new detached region. Isoenergetic contours for both branches at the magnetic fields $h \geqslant h_{c2}$ are shown. With an increase in the magnetic field the minimum $\epsilon_1^{\min}(h)$ of the branch $\epsilon = \epsilon_1$ moves up (curves 1 and 2) and at $E = \epsilon_1^{\min}(h)$ crosses the

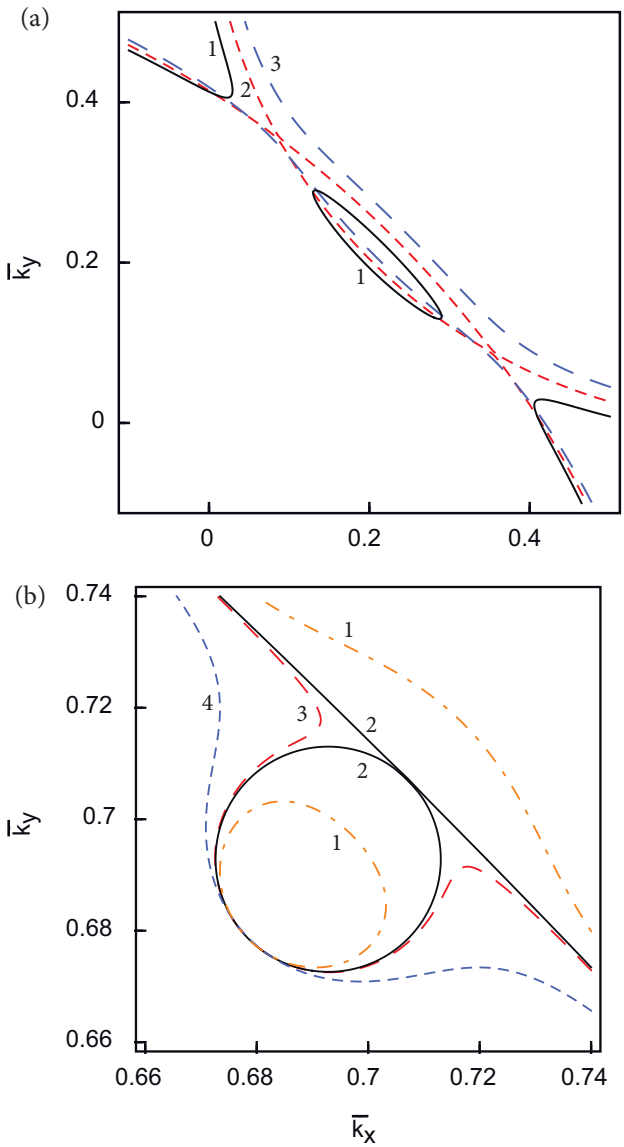

FIG. 4. Fine structure of isoenergetic contours of the branch $\epsilon = \epsilon_2$ for different magnetic fields $\bar{h} \leqslant \bar{h}_{c1} = 0.96 < \bar{h}_{c2} = 1$. (a) The energy $E \leqslant E_0$ is equal to the energy of the saddle point $\bar{E} = \bar{\epsilon}_2^{\mathrm{sad3,4}}(\bar{h} = 0.3) = 0.026\,875$ (40): $\bar{h} = 0.29$, black solid line (1); $\bar{h} = 0.3$, red short-dashed line (2); $\bar{h} = 0.31$, blue long-dashed line (3). (b) The energy $\bar{E} < E_0(h_{c1}) = 0.4608$ is equal to the energy of the saddle point $\bar{E} = \bar{\epsilon}_2^{\mathrm{sad3,4}}(\bar{h}_{c1}) = 0.4600$ (40) at the critical field $\bar{h}_{c1} = 0.96$: $\bar{h} = 0.9599$, orange dotted-dashed line (1); $\bar{h} = \bar{h}_{c1} = 0.96$, black solid line (2); $\bar{h} = 0.960\,01$, red long-dashed line (3); $\bar{h} = 0.9602$, blue short-dashed line (4). For SOI constants and magnetic field direction we used the values $\bar{\alpha} = 0.8$, $\bar{\beta} = 0.4$, $\varphi_h = 3\pi/4$.

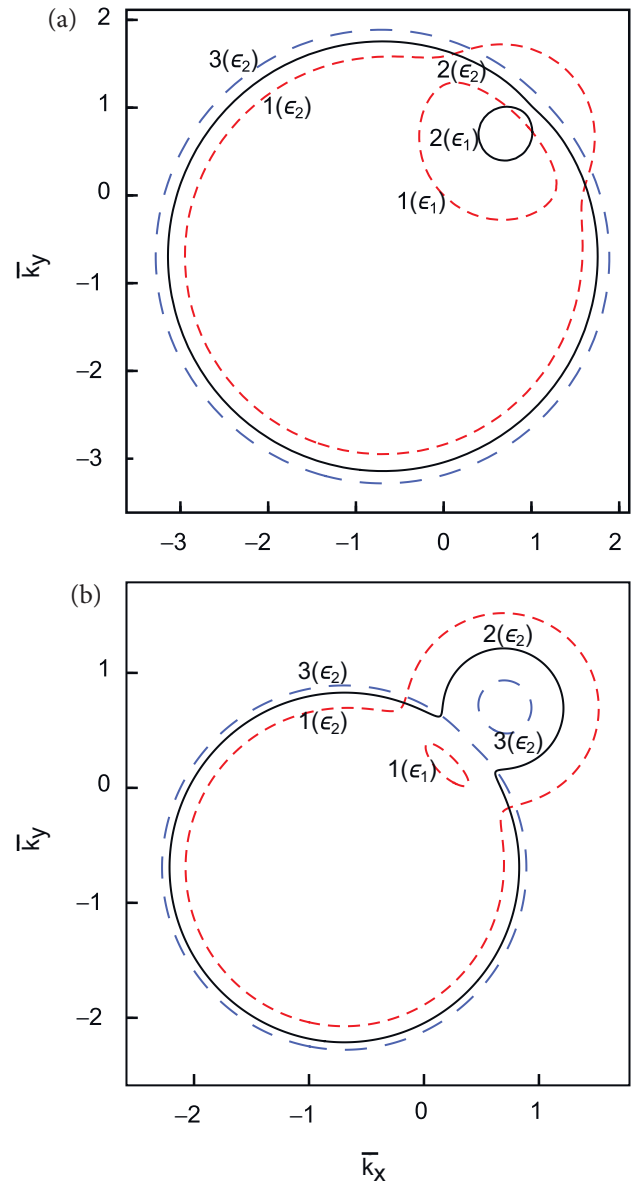

FIG. 5. (a) Isoenergetic contours for both branches (labeled in brackets) at the magnetic fields $\bar{h} \geqslant \bar{h}_{c2} = 1$ and $\bar{E} = 1$: $\bar{h} = \bar{h}_{c2}$, $\bar{E}_0 = 0.5$, $\bar{E} > \bar{\epsilon}_1^{\min} = 0.5$, red short-dashed contours (1); $\bar{h} = 1.45$, $\bar{E}_0 = 1.05$, $\bar{E} > \bar{\epsilon}_1^{\min} = 0.95$, solid contours (2); $\bar{h} = 1.8$, $\bar{E}_0 = 1.62$, $\bar{E} < \bar{\epsilon}_1^{\min} = 1.3$, blue long-dashed contours (3). (b) Isoenergetic contours for $\bar{\epsilon}_{1,2} = \bar{E} = \bar{E}_0(\bar{h} = 0.5) = 0.125$, $\bar{h} < \bar{h}_{c1} = 0.96$, $\bar{h}_{c2} = 1$: $\bar{h} = 0.3$, $\bar{E}_0 = 0.045 < \bar{E}$, red short-dashed contours (1); $\bar{h} = 0.5$, $\bar{E}_0 = 0.125 = \bar{E}$, solid contour (2); $\bar{h} = 0.6$, $\bar{E}_0 = 0.18 > \bar{E}$, blue long-dashed contours (3). For SOI constants and magnetic field direction we used the values $\bar{\alpha} = 0.8$, $\bar{\beta} = 0.4$, $\varphi_h = 3\pi/4$.

energy level. At this field the contour related to the branch $\epsilon = \epsilon_1$ disappears (curve 3). In Fig. 6(b) we show a similar topological transition at $h < h_{c2}$ when E_0 is the smallest value of the branch $\epsilon = \epsilon_1$. If $E_0 < E$, the energy spectrum consists of two electron contours (curves 1), one of which disappears at $E_0 = E$ (curve 2). In larger fields the second contour splits into two contours (curves 3), as it was shown in Fig. 5(a).

Figure 6 demonstrates the evolution of the isoenergetic contour for the magnetic field directed along the axis $k_x = k_y$ (Sec. IV B). The disruption of the neck of the contour for the energy close to the saddle point $\epsilon_2^{\mathrm{sad}}(h)$ (53) is shown in Fig. 6(a): Contour 1 corresponds to $\epsilon_2^{\mathrm{sad}}(h) < E$. The critical (self-crossing) contour 2 is in keeping with $\epsilon_2^{\mathrm{sad}}(h) = E$. In higher fields the critical contour splits up into two disconnected parts (contours 3). Figure 6(b) demonstrates the appearance of a self-crossing contour in the magnetic field at which $E_0(h) = E$.

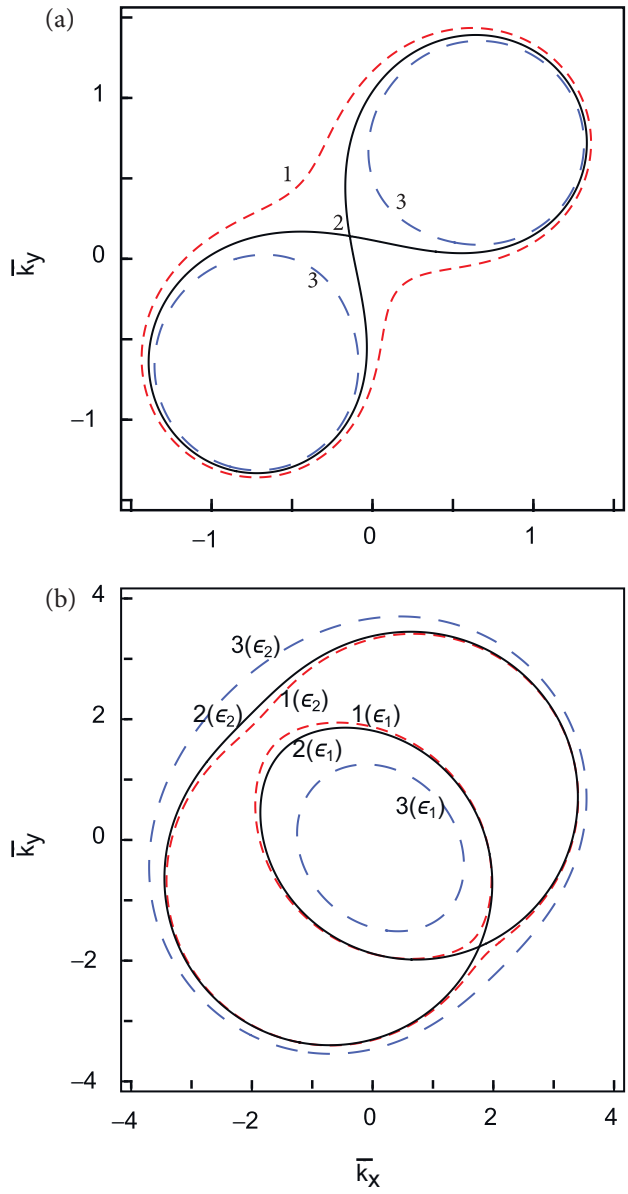

FIG. 6. (a) Isoenergetic contours for the energy $\bar{E} = \bar{\epsilon}_2^{\rm sad}(\bar{h} = 0.3) = 0.28$ (53) and $\bar{h}_{c2} = 0.04 < \bar{h} < \bar{h}_{c1} = 0.96$: $\bar{h} = 0.4$, red short-dashed contour(1); $\bar{h} = 0.3$, black solid contour (2); $\bar{h} = 0.2$, blue long-dashed contours (3). (b) Isoenergetic contours for both branches (labeled in brackets) at the energy $\bar{E} = \bar{E}_0(\bar{h} = 0.5) = 3.125$: $\bar{h} = 0.1$, red short-dashed contours (1); $\bar{h} = 0.5$, black solid contour; $\bar{h} = 2$, blue long-dashed contours (3). For SOI constants and magnetic field direction we used the values $\bar{\alpha} = 0.8$, $\bar{\beta} = 0.4$, $\varphi_h = \pi/4$.

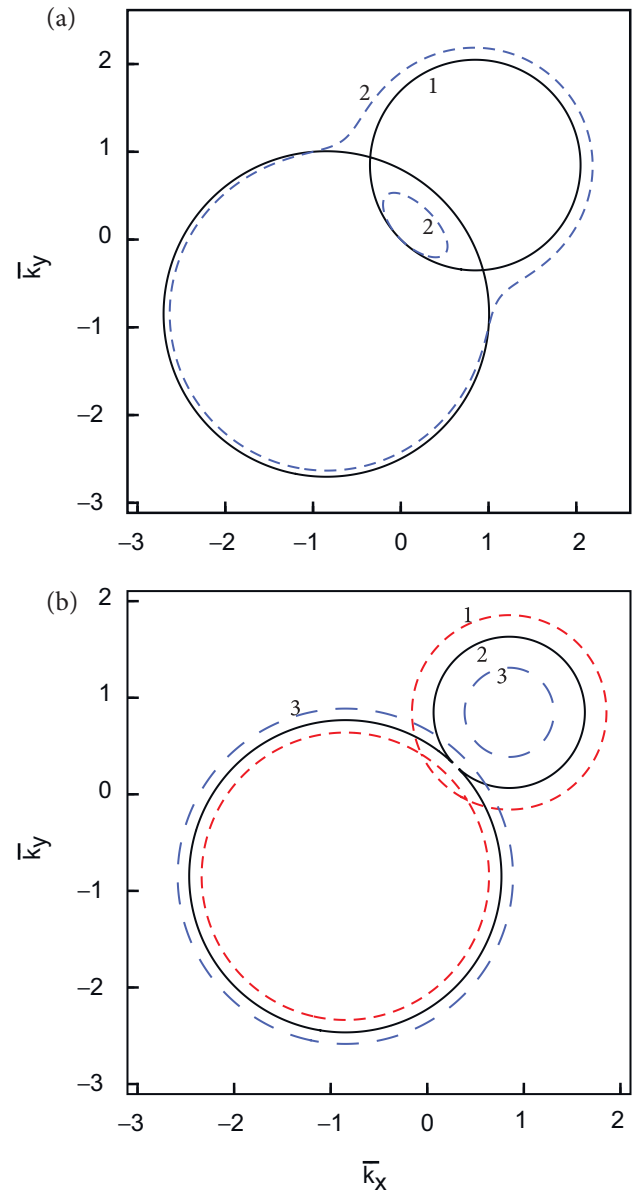

FIG. 7. (a) Isoenergetic contours at $\alpha = \beta$, $\overline{h} = 0.5$, $\overline{E} = 0.5$ for different magnetic field directions: $\varphi_h = 3\pi/4$, solid contour (1); $\varphi_h = \pi$, blue dashed contours (2). (b) Isoenergetic contours at $\varphi_h = 3\pi/4$ and for the energy corresponding to the minimum of the parabola (11) $\overline{\epsilon}_{\rm cont}^{\rm min} = \overline{E} = 0.0868$: $\overline{h} = 0.3$, red short-dashed contour (1); $\overline{h} = 0.5$, solid contour (2); $\overline{h} = 0.7$, blue long-dashed contours (3). For SOI constants we used the value $\overline{\alpha} = \overline{\beta} = 0.6$.

In Fig. 7(a), we have shown the possibility for specific changes in the topology by means of an in-plane rotation of the magnetic field in the case of equal SOI constants: The self-crossing contour (2) splits into two split-off contours (1 and 3) under a deflection of the magnetic field direction from the symmetry axis $k_x = -k_y$. Figure 7(b) shows the splitting of the self-crossing contour by the magnetic field for the energy close to the minimal energy of the branch contact points $\epsilon_{\rm cont}^{\rm min}(0, h) = \hbar^2 h^2/8m\alpha^2$ (12).

VI. SINGULARITIES IN THE ELECTRON DENSITY OF STATES

Density of state (DOS) singularities are related to the critical points of the energy spectrum. At the weak magnetic fields ($h < h_{c1}, h_{c2}$) the results (26) and (28) obtained for 2D electrons with RD SOI show that the energies of both minima and saddle points move in opposite directions on the energy scale with an increase in the value h. So, the number of Van Hove's singularities is doubled by the magnetic field. Exclusions are the directions of vector **h** along the symmetry axes when two minima (47) ($\varphi_h = \pi/4, -3\pi/4$) or two saddle

points (28) ($\varphi_h = 3\pi/4, -\pi/4$) "synchronously" move with a change in the magnetic field. In these cases the DOS has three singular points. At $h > h_{c1}$ the DOS contains two singularities which are associated with two minimum points at $h > h_{c2}$ or a minimum and saddle points at $h < h_{c2}$.

By using the coordinates (13) the DOS can be found from the relations [37]

$$\rho(E) = \frac{m}{\pi\hbar^2}, \quad E \geqslant E_0, \tag{63}$$

$$\rho(E) = \frac{m}{2\pi^2\hbar^2} \sum_{j=1,2} \oint df \frac{\lambda^{(j)}}{\sqrt{\xi^{(j)}}} \Theta(\lambda^{(j)})\Theta(\xi^{(j)}), \quad E \leqslant E_0, \tag{64}$$

where $\lambda^{(j)}$ and $\xi^{(j)}$ are defined by Eqs. (15) and (60), and $\Theta(x)$ is the Heaviside step function. Equation (63) shows that the DOS is the same as for free 2D electron gas for energies $E \geqslant E_0$. When the opposite inequality $E < E_0$, the DOS $\rho(E)$ depends on the magnetic field and constants of SOI.

One finds the electron density by integration of Eq. (64) over energies below the Fermi level E_F [37],

$$n_e = \frac{m}{\pi\hbar^2}\left[E_F + \frac{m}{2\hbar^2}(\alpha^2 + \beta^2)\right], \tag{65}$$

for $E_F \geqslant E_0$.

The Van Hove singularities of $\rho(E)$ are related to the minima and saddle points on the energy surfaces (58) and correspond to singularities in the integral (64) $\xi^{(j)}(f_\nu^{(j)}) = 0$. In order to separate the singular part of DOS near the critical point $E \to \epsilon_i^{\rm crit}$, $f \to f_\nu^{(i)}$, we use a standard way. Equation (64) can be written as a sum of a convergent and divergent parts,

$$\rho(E) = \rho_0(E) + \delta\rho(E), \tag{66}$$

$$\rho_0(E) = \frac{m}{2\pi^2\hbar^2} \sum_{j=1,2} \oint df \frac{\lambda^{(j)}(f) - \delta_{ij}\lambda^{(j)}(f_\nu^{(j)})}{\sqrt{\xi^{(j)}(f)}} \times \Theta(\lambda^{(j)})\Theta(\xi^{(j)}), \tag{67}$$

$$\delta\rho(E) = \frac{m}{2\pi^2\hbar^2}\lambda^{(i)}(f_\nu^{(i)}) \oint \frac{df}{\sqrt{\xi^{(i)}(f)}} \Theta(\lambda^{(i)})\Theta(\xi^{(i)}). \tag{68}$$

The continuous function $\xi^{(i)}(f)$ can be expanded as a Taylor series in a vicinity of the point $f = f_\nu^{(i)}$,

$$\xi^{(1,2)}(f) = (\lambda^{(1,2)})^2 + \frac{2m(E-E_0)}{\hbar^2} \simeq \frac{2m(E-\epsilon_{1,2}^{\rm crit})}{\hbar^2} + \lambda^{(1,2)}(f_\nu^{(1,2)})\ddot{\lambda}^{(1,2)}(f_\nu^{(1,2)})(f - f_\nu^{(1,2)})^2 + \frac{1}{6}\lambda^{(1,2)}(f_\nu^{(1,2)})^{(1,2)}(f_\nu^{(1,2)})(f - f_\nu^{(1,2)})^3 + \cdots. \tag{69}$$

Substituting the expansion (69) into Eq. (68) we integrate using the cutoff of the integral by the Θ functions. At $E \to \epsilon_i^{\rm crit}$ the singular term $\delta\rho(E)$ (68) does not depend on the interval of integration. As shown in Sec. III, for the energy minima $\epsilon_{1,2}^{\min}$, the second derivatives are negative, $\ddot{\lambda}^{(2)}(f_\nu^{(1,2)}) < 0$, and for the saddle points $\epsilon_2^{\rm sad}$, the second derivatives are positive, $\ddot{\lambda}^{(2)}(f_\nu^{(1,2)}) > 0$. As a result, we have in a vicinity of the minimum points

$$\delta\rho(E) = \frac{m}{2\pi\hbar^2}\sqrt{\frac{\lambda^{(1,2)}}{|\ddot{\lambda}^{(1,2)}|}}\Bigg|_{f=f_\nu^{(1,2)}} \Theta\left(E - \epsilon_{1,2}^{\min}\right). \tag{70}$$

For saddle point one finds

$$\delta\rho(E) = -\frac{m}{2\pi^2\hbar^2}\sqrt{\frac{\lambda^{(2)}}{\ddot{\lambda}^{(2)}}} \times \ln\left[\frac{2m|E - \epsilon_2^{\rm sad}|}{\hbar^2\lambda^{(2)}\ddot{\lambda}^{(2)}}\right]_{f=f_\nu^{(2)}}. \tag{71}$$

At the critical magnetic field $h = h_{c1}$ the first and second derivatives of $\lambda^{(2)}(f)$ are equal to zero, and the third term in the expansion (69) must be taken into account. The singular part of the DOS in the case of the degenerate critical point reads ($\dddot{\lambda}^{(2)} \neq 0$)

$$\delta\rho(E) = \frac{m\sqrt{6}}{2\pi^{3/2}\hbar^2}\frac{\Gamma(7/6)}{\Gamma(2/3)} \times \sqrt{\frac{\lambda^{(2)}}{|\dddot{\lambda}^{(2)}|}}\left(\frac{12m|E - \epsilon_2^{\rm crit}|}{\hbar^2\lambda^{(2)}|\dddot{\lambda}^{(2)}|}\right)^{-1/6}_{f=f_\nu^{(2)}}. \tag{72}$$

The results (70) and (71) agree with the classical results for the two-dimensional case obtained in Van Hove's paper [26]. The simple relations between the energies of the critical points and SOI constants for directions of the magnetic field along the symmetry axes (see Sec. IV) is the way to find α and β from the position of DOS singularities on the magnetic field scale.

VII. CONCLUSIONS

The evolution of the energy spectrum of 2D electron gas with combined Rashba and Dresselhaus SOI (3) under the influence of in-plane magnetic field **B** has been analyzed for arbitrary SOI constants. It has been shown that the geometry of the energy surfaces (14) and isoenergetic contours (58) can be described by means of a single function (15), which depends on the magnetic field and SOI constants. We have found the relations which describe the dependencies of the critical point energies (25) and their positions (22) in the wave-vector space on the vector **B**. There are two critical values of the magnetic field at which the essential transformation of the energy spectrum occurs: At the field $B = B_1$ (33) the minimum point and saddle point of the energy branch $\epsilon = \epsilon_2$ "annihilate" and at $B = B_2$ (32) the conical point of the branch $\epsilon = \epsilon_1$ transforms into the critical (minimum) point. Finally, the spectrum having four critical points (two minima and two saddle points) and a conical point at $B = 0$ evolves into a spectrum with two minima at $B > B_1, B_2$. The general conclusions are illustrated for the directions of vector **B** along the symmetry axes. On the basis of an analysis of the dependence of the spectrum's critical points on the magnetic field, Lifshitz topological transitions in the geometry of isoenergetic contours have been studied (Figs. 4–7). Along with critical contours related to the spectrum's critical points, the appearance (or disappearance) of self-crossing contours with a

magnetic field variation is found as well. Singular additions to the electron density of states have been derived in (70)–(72). The positions of these singularities on the magnetic field scale make it possible to find both the SOI constants. We have found a $(-1/6)$-root singularity for the degenerate critical points at $B = B_{c1}$ (72). The obtained results can be used for theoretical investigations of any kinetic and thermodynamic characteristics of 2D electrons with RD SOI in the in-plane magnetic field as well as for interpretations of experimental data.

Magnetic field driven topological transitions can be observed in the 2D electron gas with a low electron density $n \simeq 10^9$–10^{10} cm^{-2} (see, for example, Ref. [38]). In heterostructures with a higher density it could be essentially reduced by a negative gate voltage [39]. For the typical values of RD SOI constants and an effective mass for an $Al_xGa_{1-x}N/GaN$ heterostructure, $\alpha \simeq 10^{-10}$ eV cm, $\alpha/\beta \simeq 10$, $m = 0.2m_0$, $g^* = 2$ [40,41], and $n \simeq 10^{10}$ cm^{-2}, we estimate a Fermi energy, $E_F \simeq 0.1$ meV, by using Eq. (65). In this case the Van Hove singularities appear in a magnetic field $0 < B \lesssim 2$ T. Another possibility to observe the predicted topological transitions is with the in-plane tunneling spectroscopy [42–44]. While a tunneling conductance is proportional to the density of states at a shifted energy $\rho(\epsilon = E_F - eU)$, where eU is a bias energy, the electron states below the Fermi level can be investigated.

ACKNOWLEDGMENT

One of us (Yu.K.) would like to acknowledge useful discussions with S. V. Kuplevakhsky.

APPENDIX: FUNCTIONS $\lambda^{(1,2)}$ AND $\ddot{\lambda}^{(1,2)}$ IN THE CRITICAL POINTS OF ENERGY SPECTRUM $\dot{\lambda}^{(1,2)} = 0$ FOR THE MAGNETIC FIELD DIRECTED ALONG THE SYMMETRY AXIS

1. Magnetic field directed along the $k_x = -k_y$ axis

Substituting the angles (34) and (35) corresponding to the zeros of $\dot{\lambda}^{(1,2)}$, we find the functions $\lambda^{(1,2)}$ (15),

$$\lambda^{(1,2)}\left(-\frac{3\pi}{4}\right) = \mp\frac{m}{\hbar^2}(\alpha+\beta) \mp \frac{h}{\alpha+\beta}, \tag{A1}$$

$$\lambda^{(1,2)}\left(\frac{\pi}{4}\right) = \mp\frac{m}{\hbar^2}(\alpha+\beta) \pm \frac{h}{\alpha+\beta}, \tag{A2}$$

$$\lambda^{(1,2)}(f_{3,4}) = \mp\frac{m}{\hbar^2}(\alpha-\beta)\sqrt{1-\frac{h^2}{h_{c1}h_{c2}}}, \quad h \leqslant h_{c1}, \tag{A3}$$

and second derivatives $\ddot{\lambda}^{(1,2)}(f)$,

$$\ddot{\lambda}^{(1,2)}\left(-\frac{3\pi}{4}\right) = \pm\frac{h+h_{c1}}{\alpha+\beta}, \tag{A4}$$

$$\ddot{\lambda}^{(1,2)}\left(\frac{\pi}{4}\right) = \mp\frac{h-h_{c1}}{\alpha+\beta}, \tag{A5}$$

$$\ddot{\lambda}^{(1,2)}(f_{3,4}) = \mp\frac{h_{c1}}{\alpha-\beta}\left[1-\left(\frac{h}{h_{c1}}\right)^2\right] \times\sqrt{1-\frac{h^2}{h_{c1}h_{c2}}}, \quad h \leqslant h_{c1}. \tag{A6}$$

Equations (25) and (A1)–(A3) give the formulas for energies which can be possible critical points $\epsilon^{\mathrm{crit}\,\nu}(h) = \epsilon_{1,2}(f_\nu^{(1,2)})$ (25) of the energy spectrum,

$$\epsilon^{\mathrm{crit1}}(h) = -\frac{m}{2\hbar^2}(\alpha+\beta)^2 - h,$$

$$\epsilon^{\mathrm{crit2}}(h) = -\frac{m}{2\hbar^2}(\alpha+\beta)^2 + h, \tag{A7}$$

$$\epsilon^{\mathrm{crit3,4}}(h) = -\frac{m}{2\hbar^2}(\alpha-\beta)^2 + \frac{h^2\hbar^2}{8m\alpha\beta}. \tag{A8}$$

2. Magnetic field directed along the $k_x = k_y$ axis

The functions $\lambda^{(1,2)}$ in the points (44) of the first derivatives $\dot{\lambda}^{(1,2)}$ zeros are given by

$$\lambda^{(1,2)}\left(\frac{3\pi}{4}\right) = \mp\frac{m}{\hbar^2}(\alpha-\beta) + \frac{h}{\alpha-\beta}, \tag{A9}$$

$$\lambda^{(1,2)}\left(-\frac{\pi}{4}\right) = \mp\frac{m}{\hbar^2}(\alpha-\beta) - \frac{h}{\alpha-\beta}, \tag{A10}$$

$$\lambda^{(1,2)}(f_{3,4}) = \mp\frac{m}{\hbar^2}(\alpha+\beta)\sqrt{1+\frac{h^2}{h_{c1}h_{c2}}}, \quad h \leqslant h_{c1}, \tag{A11}$$

and their second derivatives $\ddot{\lambda}^{(1,2)}$ read

$$\ddot{\lambda}^{(1,2)}\left(\frac{3\pi}{4}\right) = -\frac{h-h_{c1}}{\alpha-\beta}, \tag{A12}$$

$$\ddot{\lambda}^{(1,2)}\left(-\frac{\pi}{4}\right) = \frac{h+h_{c1}}{\alpha-\beta}, \tag{A13}$$

$$\ddot{\lambda}^{(1,2)}(f_{3,4}) = \pm\frac{h_{c1}}{\alpha+\beta}\left[1-\left(\frac{h}{h_{c1}}\right)^2\right] \times\sqrt{1+\frac{h^2}{h_{c1}h_{c2}}}, \quad h \leqslant h_{c1}. \tag{A14}$$

As the last step one must separate the physical solutions: Only the positive values of $\lambda^{(1,2)}(f_\nu^{(1,2)})$ satisfy Eq. (20). From the simple analysis of Eqs. (A1)–(A14) we obtain conditions of the existence of extrema in different ranges of the magnetic field.

[1] I. M. Lifshitz, Sov. Phys. JETP **11**, 1130 (1960).
[2] I. M. Lifshits, M. Ya. Azbel', and M. I. Kaganov, *Electron Theory of Metals* (Consultants Bureau, New York, 1973).
[3] A. A. Varlamov, V. S. Egorov, and A. V. Pantsulaya, Adv. Phys. **38**, 469 (1989).
[4] Ya. M. Blanter, M. I. Kaganov, A. V. Pantsulaya, and A. A. Varlamov, Phys. Rep. **245**, 159 (1994).

[5] G. E. Volovik, Low Temp. Phys. **43**, 47 (2017); Usp. Fiz. Nauk **188**, 95 (2018).

[6] A. Manchon, H. C. Koo, J. Nitta, S. M. Frolov, and R. A. Duine, Nat. Mater. **14**, 871 (2015).

[7] D. Bercioux and P. Lucignano, Rep. Prog. Phys. **78**, 106001 (2015).

[8] I. I. Boiko and E. I. Rashba, Sov. Phys. Solid State **2**, 1692 (1961).

[9] G. A. H. Schober, H. Murakawa, M. S. Bahramy, R. Arita, Y. Kaneko, Y. Tokura, and N. Nagaosa, Phys. Rev. Lett. **108**, 247208 (2012).

[10] L. Meier, G. Salis, I. Shorubalko, E. Gini, S. Scho, and K. Ensslin, Nat. Phys. **3**, 650 (2007).

[11] Y. F. Hao, Eur. Phys. J. B **85**, 84 (2012).

[12] L. G. D. da Silveira, P. Barone, and S. Picozzi, Phys. Rev. B **93**, 245159 (2016).

[13] M. Kepenekian and J. Even, J. Phys. Chem. Lett. **8**, 3362 (2017).

[14] S. D. Ganichev and L. E. Golub, Phys. Status Solidi B **251**, 1801 (2014).

[15] C. M. Wang, Phys. Rev. B **82**, 165331 (2010).

[16] M. A. Wilde and D. Grundler, New J. Phys. **15**, 115013 (2013).

[17] D. H. Berman and M. E. Flatte, Phys. Rev. Lett. **105**, 157202 (2010).

[18] S. M. Badalyan, A. Matos-Abiague, G. Vignale, and J. Fabian, Phys. Rev. B **81**, 205314 (2010).

[19] I. V. Kozlov and Yu. A. Kolesnichenko, Low Temp. Phys. **43**, 855 (2017).

[20] R. Winkler, *Spin-Orbit Coupling Effects in Two-Dimensional Electron and Hole Systems* (Springer, Berlin, 2003).

[21] Yu. V. Pershin, J. A. Nesteroff, and V. Privman, Phys. Rev. B **69**, 121306(R) (2004).

[22] Yu. Ya. Tkach, JETP Lett. **104**, 105 (2016).

[23] O. N. Shevchenko and A. I. Kopeliovich, Low Temp. Phys. **42**, 196 (2016).

[24] P. S. Alekseev, M. V. Yakunin, and I. N. Yassievich, Semiconductors **41**, 1092 (2007).

[25] V. A. Sablikov and Yu. Ya. Tkach, Phys. Rev. B **99**, 035436 (2019).

[26] L. Van Hove, Phys. Rev. **89**, 1189 (1953).

[27] K. Wolff, R. Schafer, M. Meffert, D. Gerthsen, R. Schneider, and D. Fuchs, Phys. Rev. B **95**, 245132 (2017).

[28] R. Eppenga and M. F. H. Schuurmans, Phys. Rev. B **37**, 10923 (1988).

[29] A. M. Gilbertson, M. Fearn, J. H. Jefferson, B. N. Murdin, P. D. Buckle, and L. F. Cohen, Phys. Rev. B **77**, 165335 (2008).

[30] P. Kleinert and V. V. Bryksin, Phys. Rev. B **76**, 205326 (2007).

[31] W. Xu and Y. Guo, Phys. Lett. A **340**, 281 (2005).

[32] E. I. Rashba, Sov. Phys. Solid State **2**, 1109 (1960); Yu. A. Bychkov, and E. I. Rashba, JETP Lett. **39**, 78 (1984).

[33] G. Dresselhaus, Phys. Rev. **100**, 580 (1955).

[34] J. Nitta, T. Akazaki, and H. Takayanagi, Phys. Rev. Lett. **78**, 1335 (1997).

[35] Y. Sato, T. Kita, S. Gozu, and S. Yamada, J. Appl. Phys. **89**, 8017 (2001).

[36] A. J. A. Beukman, F. K. de Vries, J. van Veen, R. Skolasinski, M. Wimmer, F. Qu, D. T. de Vries, B. M. Nguyen, W. Yi, A. A. Kiselev, M. Sokolich, M. J. Manfra, F. Nichele, C. M. Marcus, and L. P. Kouwenhoven, Phys. Rev. B **96**, 241401 (2017).

[37] I. V. Kozlov and Yu. A. Kolesnichenko, Phys. Lett. A **383**, 764 (2019).

[38] J. Zhu, H. L. Stormer, L. N. Pfeiffer, K. W. Baldwin, and K. W. West, Phys. Rev. Lett. **90**, 056805 (2003).

[39] C. Rossler, T. Feil, P. Mensch, T. Ihn, K. Ensslin, D. Schuh, and W. Wegscheider, New J. Phys. **12**, 043007 (2010).

[40] C. Yin, B. Shen, Q. Zhang, F. Xu, N. Tang, L. Cen, X. Wang, Y. Chen, and J. Yu, Appl. Phys. Lett. **97**, 181904 (2010).

[41] W. Knap, E. Frayssinet, and M. L. Sadowski, C. Skierbiszewski, D. Maude, V. Falko, M. Asif Khan, and M. Asif Khan, Appl. Phys. Lett. **75**, 3156 (1999).

[42] Y. S. Ang, Z. Ma, and C. Zhang, Sci. Rep. **4**, 3780 (2014).

[43] B. Srisongmuang, P. Pairor, and M. Berciu, Phys. Rev. B **78**, 155317 (2008).

[44] A. Jantayod and P. Pairor, Physica E **48**, 111 (2013).